Band-Limited Volterra Series-Based Digital Predistortion for Wideband RF Power Amplifiers

Chao Yu, *Student Member*, *IEEE*, Lei Guan, *Student Member*, *IEEE*, Erni Zhu, and Anding Zhu, *Member*, *IEEE*

***Abstract*— The continuously increasing demand for wide bandwidth creates great difficulties in employing digital predistortion (DPD) for radio frequency (RF) power amplifiers (PAs) in future ultra wideband systems because the existing DPD system requires multiple times the input signal bandwidth in the transmitter and receiver chain, which is sometimes almost impossible to implement in practice. In this paper, we present a novel band-limited digital predistortion technique in which a band-limiting function is inserted into the general Volterra operators in the DPD model to control the signal bandwidth under modeling, which logically transforms the general Volterra series-based model into a band-limited version. This new approach eliminates the system bandwidth constraints of the conventional DPD techniques, and it allows users to arbitrarily choose the bandwidth to be linearized in the PA output according to the system requirement without sacrificing performance, which makes the DPD system design much more flexible and feasible. In order to validate this idea, a high power LDMOS Doherty PA excited by various wideband signals, including 100 MHz LTE-Advanced signals, was tested. Experimental results showed that excellent linearization performance can be obtained by employing the proposed approach. Furthermore, this technique can be applied to other linear-in-parameter models. In future ultra wideband systems, this new technique can significantly improve system performance and reduce DPD implementation cost.**

***Index Terms*—Behavioral model, digital predistortion, linearization, LTE-Advanced, power amplifiers, Volterra series.**

I. Introduction

In order to satisfy growing demands for high data rates and large capacity, transmit signal bandwidth is continuously increasing in modern wireless communication systems. For example, 100 MHz instantaneous modulation bandwidth will be required in the forthcoming Long Term Evolution Advanced (LTE-Advanced) systems [1]. This demanding bandwidth requirement creates great difficulties in designing radio frequency (RF) power amplifiers (PAs) to meet efficiency specifications while simultaneously conforming to spectral mask and in-band distortion requirements. Digital predistortion (DPD) is one of the advanced linearization techniques that compensates for nonlinear distortion in RF PAs by inverting their nonlinear behavior using digital circuits [2]. DPD allows PAs to be operated at higher drive levels for higher efficiency without sacrificing linearity, which is nowadays one of the essential units in high power wireless base stations [3].

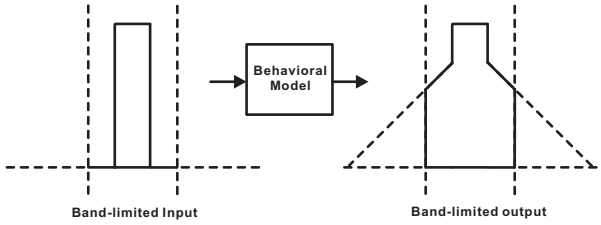

Fig. 1. Band-limited input and output.

It is well known that the RF power amplifier is inherently nonlinear, and it produces in-band distortion and inter-modulation products that cause spectral regrowth in the adjacent channels. For a modulated signal, fifth-order products appear within a range of five times the bandwidth of the input signal. In order to accurately model and effectively linearize the RF PA, an output signal occupying multiple times the input bandwidth, usually five times, is required to be captured. In the past decades, many DPD models have been developed [4]-[15]. Among them, truncated Volterra series-based models, such as memory polynomial (MP) [5], generalized memory polynomial (GMP) [6], and dynamic deviation reduction-based Volterra series (DDR) [7], are very popular. These models are based on polynomial-type of functions, of which the output bandwidth increases proportionally with the nonlinear orders. This property can effectively match the nonlinear behavior of the RF PAs, and hence these models work very well in the existing systems.

However, in the forthcoming wideband system, e.g., LTE-Advanced, 100 MHz modulation bandwidth is required, which means that 500 MHz linearization bandwidth will be required if the existing DPD techniques are employed. Such a wide bandwidth requirement will remarkably increase the difficulties in system design. It requires not only very high speed data converters but also ultra wideband transmitter and receiver chains, which make DPD sometimes become infeasible. On the other hand, in practice, it may not be necessary to linearize the PA up to such a wideband bandwidth because the signal bandwidth is expanded too wide. We may

This is an expanded paper from the IEEE MTT-S Int. Microwave Symposium held on June 17-22, 2012 in Montreal, Canada. This work was supported by the Science Foundation Ireland under the Principal Investigator Award scheme, and in part by Huawei Technologies Co. Ltd.

C. Yu, L. Guan and A. Zhu are with the School of Electrical, Electronic and Communications Engineering, University College Dublin, Dublin 4, Ireland (e-mail: chao.yu@ucdconnect.ie; lei.guan@ucd.ie; anding.zhu@ucd.ie).

E. Zhu is with Huawei Technologies Co. Ltd., Shanghai, China (e-mail: erni_zhu@huawei.com).

only need to remove the distortion near the input center frequency band, e.g., within 200 to 300 MHz range. The distortion beyond that band can be filtered by using a bandpass filter at the PA output, or it may have already been taken care of by the cavity filters in the duplexer. Therefore, in the future system, we may face a scenario that only the distortion within a limited bandwidth is captured, as illustrated in Fig. 1, and we only need to linearize the system within that limited bandwidth. In this new scenario, however, the conventional DPD models can no longer be employed. This is because almost all of the existing models are constructed in the time domain with very little or no control in the frequency domain. For instance, in the MP model, the bandwidth of the frequency domain signal solely depends on the nonlinear order selected and the distortion resulted from each nonlinear operation are spread over the corresponding bandwidth. However, in the new system, as shown in Fig. 1, only distortion within a limited bandwidth is captured and the rest of distortion is missing, which leads that the signal bandwidth produced by the model does not match the bandwidth of the system under modeling, and thus the model accuracy may be significantly decreased, so that the linearization performance can be deteriorated.

In [16], a band-limited Volterra series-based behavioral modeling approach was proposed, which allows us to accurately model a PA with band-limited input and output. This is achieved by inserting a band-limiting function into each Volterra operator before multiplying with its coefficients. By controlling the bandwidth of the band-limiting function, we can arbitrarily choose the bandwidth under modeling. It naturally transforms the general Volterra series-based models into band-limited ones. This approach eliminates the inherent bandwidth requirement of the general Volterra series but still keeps the same model structure, such as the linear-in-parameter property. Experimental results showed that the proposed approach significantly improves the model accuracy.

In this paper, we introduce a band-limited DPD system by employing the proposed modeling technique. In this new system, the DPD bandwidth can be arbitrarily chosen according to the system requirement, which removes the system bandwidth constrains of the conventional system. It provides an extra freedom for DPD designers to make tradeoffs between linearization bandwidth and system cost. Detailed theoretical analysis and rigorous experimental validations are presented in the paper.

The paper is organized as follows. In Section II, we briefly re-introduce the band-limited behavioral modeling methodology proposed in [16]. A band-limited DPD system is then proposed in Section III while the model implementation is presented in Section IV. Experimental results are given in Section V with a conclusion in Section VI.

II. Band-limited Behavioral Modeling

A. General Volterra Series

In the discrete time domain, a general Volterra series [17] can be written as

$$y(n)=\sum_{p=1}^{\infty}\sum_{i_1=0}^{\infty}\cdots\sum_{i_p=0}^{\infty}h_p(i_1,\cdots,i_p)D_p[x(n)] \tag{1}$$

where $x(n)$ and $y(n)$ represents the input and output, respectively, $h_p(i_1,\cdots,i_p)$ is the pth-order Volterra kernel and

$$D_p[x(n)]=\prod_{j=1}^{p}x(n-i_j) \tag{2}$$

where D_p is the pth-order Volterra operator. In a real application, the general Volterra series is normally simplified to a certain format. For instance, only limited dynamic orders are considered in the DDR-Volterra model [7]. One of the main advantages of the Volterra models is that the output of the model is linear with respect to its coefficients, meaning that it is possible to extract a nonlinear Volterra model in a direct way by using linear system identification algorithms, such as least squares (LS).

However, one common feature of these models is that the signal bandwidth in the frequency domain increases with the nonlinear orders involved in the model. As shown in Fig. 2, when the input signal passes each nonlinear Volterra operator, the signal bandwidth proportionally increases with the order of nonlinearity selected. For example, the 3rd-order operator will expand the signal bandwidth 3 times, and the final output bandwidth depends on the highest order of nonlinearity chosen. Sufficient accuracy can be achieved when the nonlinear order in the model matches the bandwidth of the system under modeling. For instance, a 5th-order model can be used when the output signal within five times the input signal bandwidth is captured. However, in the wideband scenario described earlier, the output signal may be filtered before it is captured. In that case, although the high order nonlinear distortion is spread over a wide bandwidth, only part of distortion within the filter passband is obtained while the other part is missing. If we still use the Volterra model to map the input to the output, the model accuracy will decrease because the signal bandwidth of the model does not match the signal bandwidth under modeling.

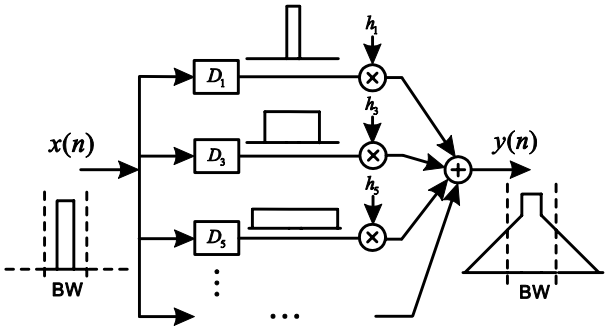

Fig. 2. General Volterra series model.

B. Proposed Band-limited Volterra Series

To resolve the bandwidth mismatch problem, a new model called *band-limited Volterra series* was proposed [16], in which a band-limiting function is introduced to control the bandwidth expansion when the signal passes each nonlinear Volterra operator. As shown in Fig. 3, a band-limiting function, $w(\cdot)$, is inserted into the Volterra operator. This band-limiting function can be a linear filter, and it can be pre-designed in the frequency domain with an effective bandwidth chosen according to the bandwidth requirement of the system output. It is then

converted into the time domain and represented by a finite impulse response. The new pth-order band-limited Volterra operator T_p can be represented by

$$T_p[x(n)] = D_p[x(n)] * w(n) \tag{3}$$

where * represents the convolution operation. The general Volterra series can thus be transformed into a band-limited version as

$$\begin{aligned} y(n) &= \sum_{p=1}^{\infty}\sum_{i_1=0}^{\infty}\cdots\sum_{i_p=0}^{\infty} h_{p,BL}(i_1,\cdots,i_p)T_p[x(n)] \\ &= \sum_{p=1}^{\infty}\sum_{i_1=0}^{\infty}\cdots\sum_{i_p=0}^{\infty} h_{p,BL}(i_1,\cdots,i_p)\left\{D_p[x(n)] * w(n)\right\} \\ &= \sum_{p=1}^{\infty}\sum_{i_1=0}^{\infty}\cdots\sum_{i_p=0}^{\infty} h_{p,BL}(i_1,\cdots,i_p)\left\{\sum_{k=0}^{K}\left[\prod_{j=1}^{p} x(n-i_j-k)w(k)\right]\right\} \end{aligned} \tag{4}$$

where T_p is the pth-order band-limited Volterra operator, $w(\cdot)$ is the band-limiting function with length K, $h_{p,BL}(i_1,\cdots,i_p)$ is the pth-order band-limited Volterra kernel, and $x(n)$ and $y(n)$ represents the input and output, respectively. As shown in Fig. 3, because the signal is filtered by the band-limiting function after it passes each Volterra operator, the bandwidth of the output from each Volterra operator is limited within a certain frequency range, e.g., BW. After linearly scaled by the coefficients and recombined together, the final output $y(n)$ is logically band-limited to BW. It allows the bandwidth of the signal produced by the model to perfectly match that of the actual PA output if BW is chosen to be equal to the bandwidth of the PA output. The accuracy of the model is therefore significantly increased. Although linear convolution is required, the model structure is still the same as that of the general Volterra series, e.g., the output is still linear with respect to the model parameters. The coefficients can therefore also be extracted by using linear system identification algorithms.

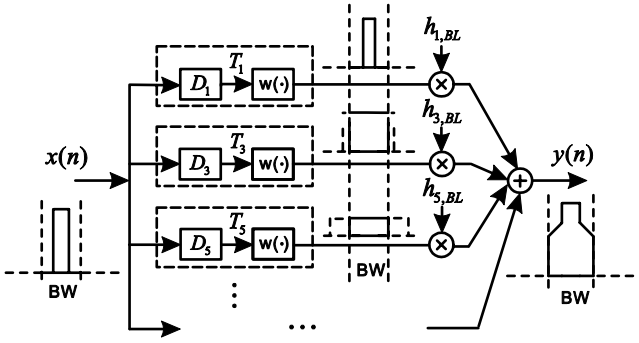

Fig. 3. Band-limited Volterra series model.

By inserting a band-limiting function into each Volterra operator, the general Volterra series is naturally transformed into the band-limited version. This intervention to the model completely changes the model behavior and significantly enhances its modeling capability. In the conventional model, there is no control in the frequency domain and the bandwidth of the output is solely decided by the nonlinear order chosen. In the new model, an extra control or freedom is obtained, namely, we can arbitrarily control the signal bandwidth produced by the model in the frequency domain by selecting different bandwidths of the band-limiting function, despite the model is still operated in the time domain. In this case, no matter how narrow the bandwidth of the PA output is, the relationship between the input and output can always be accurately represented by the new model if the bandwidth of the band-limiting function matches that of the PA output. If we consider integrating the band-limiting function with the original Volterra operator together, we can treat the new nonlinear operation (Volterra + filtering) as a new basis function. The model based on the new band-limited basis function can be used to represent a wide range of nonlinear systems, including the general Volterra series if the filter bandwidth is set to infinite. In this sense, the general Volterra series can be treated as one of special cases of the new model.

III. Band-limited Digital Predistortion

The band-limited modeling idea proposed in Section II looks very simple. However, it not only just improves the model accuracy, but also significantly enhances the modeling capability. If employed in digital predistortion, it dramatically changes the way the DPD system is operated, as we will discuss below.

A. Conventional DPD

In the conventional systems, behavioral models developed for RF PAs can be directly employed in digital predistortion and the indirect learning approach [18][19] is normally used for model extraction. It is based on the theory of the pth-order inverse described in the classical Volterra series book [17], which states that the pth-order post-inverse is the same as its pth-order pre-inverse when a nonlinear system is linearized up to the pth-order nonlinearity. In these systems, an identical model is normally used for both the pre-inverse in predistortion and the post-inverse in model extraction. In the model extraction, the output of the PA $y(n)$ is used as input of the model while the input of the PA $x(n)$ is used as the expected output. The extracted coefficients are then directly copied to the pre-inverse model, i.e., the predistortion block, as illustrated in Fig. 4. If $z(n)$ approaches $u(n)$, $y(n)$ is then close to $x(n)$.

As mentioned earlier, a signal passing a nonlinear PA will generate spectrum regrowth, and the nonlinear operators in the DPD model also expand the signal bandwidth. In the frequency domain, we can see the signal bandwidth changes when the signal passes each nonlinear block, as illustrated in Fig. 4: (i) in the post-inverse case, when the original input signal passes the PA, the bandwidth of the signal is expanded 5 times, and then after the post-inverse, the signal bandwidth returns to the original bandwidth; (ii) in the pre-inverse case, the signal bandwidth is expanded 5 times when the signal passes the predistorter block, and then returns to the original after passing the PA. In a real system, DPD is normally operated in digital baseband. The block diagram of a general DPD system is shown in Fig. 5. In order to accommodate the frequency domain characteristics and achieve high linearization performance, a general rule of thumb is that five times the input signal bandwidth would be required in both the feedback path and the transmitter chain.

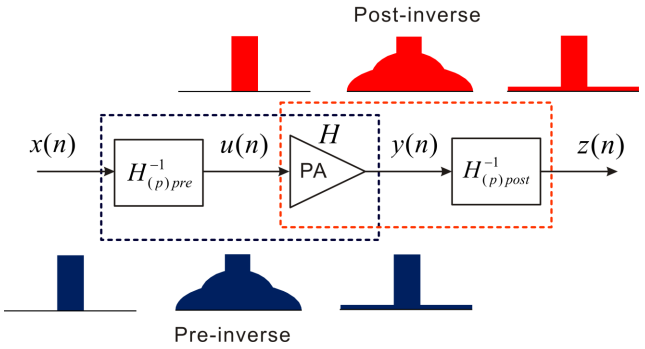

Fig. 4. Cascaded nonlinear system.

The configuration in Fig. 5 works very well in a relatively narrow band system. However, for a wideband system, e.g., the LTE-Advanced system, 100 MHz input bandwidth will be required. If the existing DPD system is used, 500 MHz linearization bandwidth will be needed. It creates enormous difficulties in real implementation. In the feedback path, a wideband down-conversion chain is required and a 500 MSPS (Mega-samples per second) sampling rate will be required for the analog-to-digital converters (ADCs) for I/Q signals[1]. If digital intermediate frequency (IF) signal is used, it will require 1 GSPS (Giga-samples per second) sampling. In order to produce the 500 MHz predistorted signal and allow it passing through the transmitter chain before feeding into the PA, very high speed digital-to-analog converters (DACs) and a wideband transmitter chain will also be required. This is very difficult and sometimes impossible to implement in practice.

On the other hand, it may not be necessary to clean up all the distortions in such a wide bandwidth by using DPD. Because when the distortion is spread into such a wide bandwidth, some distortions in the sideband can be easily filtered by using a bandpass filter in the output of the RF PA and this bandpass filter may have already existed in the transmitter, e.g., the cavity filter in the duplexer. Therefore, in practice, it would be desirable to have a DPD system that only requires limited bandwidth and only linearizes the PA up to a certain bandwidth. However, this will require necessary changes in the existing DPD models; otherwise the system performance will deteriorate quickly. It is because that the model accuracy is

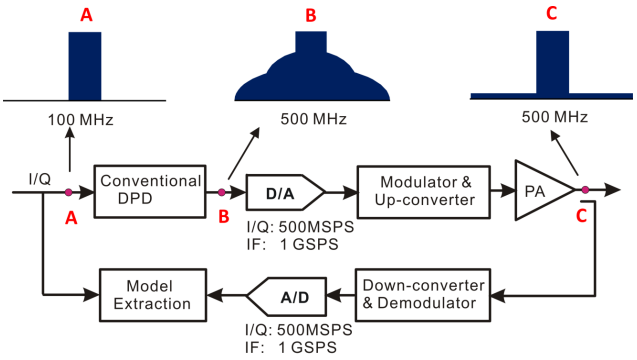

Fig. 5. Conventional DPD.

[1] The ADC sampling rate may be reduced by employing the under-sampling approach proposed in [8], but the anti-aliasing filter in the ADC must be re-designed to preserve the full sideband information, and it still requires a wideband down-conversion chain in the feedback path.

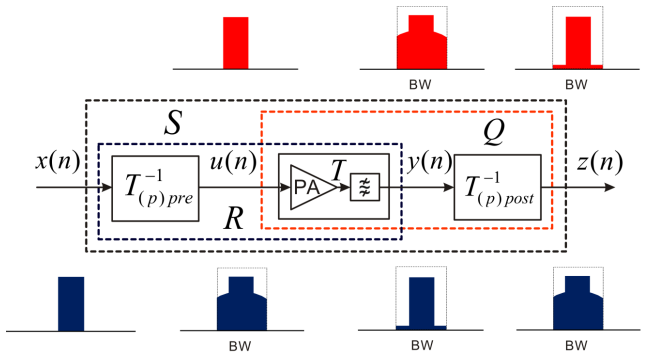

Fig. 6. Band-limited cascaded nonlinear system.

significantly reduced, when the bandwidth of the system under modeling does not match the signal bandwidth of the model, as discussed in Section II.

B. Proposed Band-limited DPD

If the band-limited model proposed in Section II is employed, the bandwidth mismatch problem can be easily resolved. Assuming that the output of the PA is filtered, the system under modeling can be represented by a nonlinear PA with a bandpass filter, as represented by T shown in Fig. 6. If we let the bandwidth of the band-limiting function equal to the bandwidth of the bandpass filter, the relationship between the PA input and output can be accurately modeled by employing the band-limited model. Because part of the frequency information is missing, invertibility of the model must be investigated before employing it in DPD. First, let's look at how the signal is handled by the model. In the PA modeling (the forward model), because we changed the basis function of the model, the frequency bandwidth of the model can now perfectly match the bandwidth of the system under modeling. With correct model extraction, the input and output relationship can be accurately represented by a *p*th-order band-limited Volterra model. Despite each of the new Volterra operator only takes into account the information within the selected bandwidth, there must be one to one mapping from the input to the output in the transfer function, the same as that in the general Volterra series. For instance, the 3rd-order basis function exactly represents the mapping from the original input to the band-limited 3rd-order distortion. Therefore, in an inverse order, if the same band-limited model structure is used and with the same signal bandwidth, the one to one mapping can of course be inversed back in the same way. The model hence indeed is invertible.

Secondly, we should discuss whether or not the *p*th-order inverse is still applicable. Let's re-derive the equations in the *p*th-order inverse theory [17]. As illustrated in Fig. 6, we simply cascade the three systems together, similar to that in Fig. 4. We first construct a *P*th-order post-inverse, $T^{-1}_{(P)post}$,with a band-limited model, and then copy it into the pre-inverse, $T^{-1}_{(P)pre}$. Let's assume

$$T^{-1}_{(P)pre} = T^{-1}_{(P)post} = T^{-1}_{(P)}. \tag{5}$$

In the system Q with the post-inverse,

$$z(n) = Q[u(n)] = u(n) + \sum_{p=P+1}^{\infty} Q_p[u(n)] \tag{6}$$

where Q_p is the pth-order band-limited Volterra operator with the post-inverse, and in the pre-inverse,

$$u(n) = T_{(P)}^{-1}[x(n)] = \sum_{p=1}^{P} T_p^{-1}[x(n)]. \tag{7}$$

So that,

$$z(n) = \sum_{p=1}^{P} T_p^{-1}[x(n)] + \sum_{p=P+1}^{\infty} Q_p[u(n)]. \tag{8}$$

Because the bandwidths of all three nonlinear systems are limited within the selected bandwidth, the overall system S can also be represented by a band-limited Volterra model as

$$z(n) = S[x(n)] = \sum_{p=1}^{\infty} S_p[x(n)] \tag{9}$$

where S_p is the pth-order band-limited Volterra operator. From (8) and (9), we can obtain,

$$S_p[x(n)] = T_p^{-1}[x(n)] \quad 1 \le p \le P. \tag{10}$$

Let's look at the first order term,

$$z_1(n) = S_1[x(n)] = T_1^{-1}[x(n)], \tag{11}$$

and in the mean time, in the post-inverse,

$$z_1(n) = T_1^{-1}[y_1(n)] \tag{12}$$

where $z_1(n)$ and $y_1(n)$ represents the first order term of $z(n)$ and $y(n)$, respectively. Comparing (11) with (12) we can obtain,

$$y_1(n) = x(n). \tag{13}$$

For the second order term, in the post-inverse,

$$z_2(n) = T_1^{-1}[y_2(n)] + T_2^{-1}[y_1(n)]. \tag{14}$$

Using (13), we obtain

$$z_2(n) = T_1^{-1}[y_2(n)] + T_2^{-1}[x(n)]. \tag{15}$$

And using (10),

$$z_2(n) = S_2[x(n)] = T_2^{-1}[x(n)]. \tag{16}$$

Comparing (15) with (16), we obtain

$$T_1^{-1}[y_2(n)] = 0. \tag{17}$$

And thus

$$y_2(n) = 0. \tag{18}$$

Following the same procedure, we can obtain

$$y_p(n) = 0 \quad p = 2, \cdots, P. \tag{19}$$

Finally, we can obtain

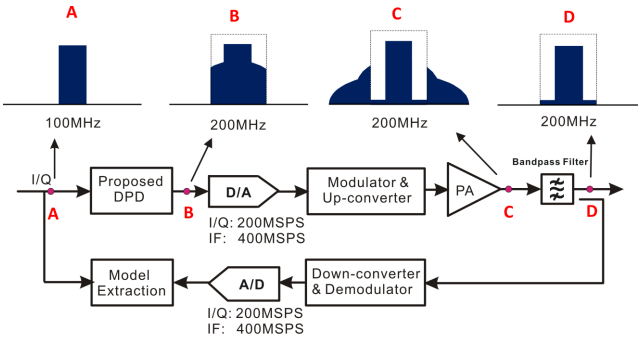

Fig. 7. Band-limited DPD.

$$y(n) = x(n) + \sum_{p=P+1}^{\infty} R_p[x(n)] \tag{20}$$

where R_p is the pth-order band-limited Volterra operator of the system R with the pre-inverse. It shows that, if $z(n)$ approaches $u(n)$, $y(n)$ is also close to $x(n)$ within the Pth-order nonlinearity, which means that the pth-order inverse is still applicable in this band-limited system. Because there is no explicit designation of bandwidth constraints in the above derivation, we can also conclude that the selected DPD bandwidth does not affect the linearization performance as long as the bandwidth of the DPD matches that of the PA output. In other words, no matter how narrow the linearization bandwidth is, the distortion within the selected bandwidth will always be reduced to the same level. The minimum bandwidth of the DPD would be the input signal bandwidth.

Based on the analysis above, a new DPD system can be constructed as shown in Fig. 7. Compared to the conventional system in Fig. 5, only two changes need to be made: (i) a bandpass filter is used in the PA output; (ii) a band-limiting function is inserted into the DPD model to control the linearization bandwidth that must match the bandwidth of the bandpass filter at the PA output. In this new system, the DPD bandwidth can be arbitrarily chosen according to the system requirement. For instance, if we only want to linearize up to 200 MHz for the 100 MHz input signal illustrated in Fig. 7, we can simply set the bandpass filter bandwidth to 200 MHz and filter out the out of band distortion before capture the 200 MHz signal in the observation path. In the transmitter chain, only 200 MHz predistorted signal is transmitted. The sampling rate of the data converters is thus reduced to 200 MSPS for I/Q signals and 400 MSPS for digital IF. Although there are still distortions in the PA output beyond 200 MHz after digital predistortion, these distortions can be filtered by the bandpass filter, and the original signal is restored in the final output. In summary, the new band-limited modeling methodology provides an additional freedom for users to choose the bandwidth to be linearized when designing a DPD system, which eliminates the system bandwidth constraints. It can significantly improve the system performance and reduce the cost of the overall system.

IV. DPD Implementation

After introducing the general structure of the band-limited DPD, we now move to model construction and parameter extraction.

A. Model Construction

The proposed band-limited modeling approach can be applied to any linear-in-parameter models. In this work, we use the simplified second-order DDR-Volterra model [20] as an example. The original DPD function is written as

$$\begin{aligned}\tilde{u}(n) = &\sum_{p=0}^{(P-1)/2}\sum_{i=0}^{M}\tilde{g}_{2p+1,1}(i)\left|\tilde{x}(n)\right|^{2p}\tilde{x}(n-i)\\ &+\sum_{p=1}^{(P-1)/2}\sum_{i=1}^{M}\tilde{g}_{2p+1,2}(i)\left|\tilde{x}(n)\right|^{2(p-1)}\tilde{x}^2(n)\tilde{x}^*(n-i)\\ &+\sum_{p=1}^{(P-1)/2}\sum_{i=1}^{M}\tilde{g}_{2p+1,3}(i)\left|\tilde{x}(n)\right|^{2(p-1)}\tilde{x}(n)\left|\tilde{x}(n-i)\right|^2\\ &+\sum_{p=1}^{(P-1)/2}\sum_{i=1}^{M}\tilde{g}_{2p+1,4}(i)\left|\tilde{x}(n)\right|^{2(p-1)}\tilde{x}^*(n)\tilde{x}^2(n-i)\end{aligned} \tag{21}$$

where $\tilde{x}(n)$ and $\tilde{u}(n)$ represents the complex envelopes of the input and output, respectively. $\tilde{g}_{2p+1,j}(\cdot)$ is the complex Volterra kernel of the system, P is the order of nonlinearity and P is an odd number, and M is the memory length.

In the band-limited system, a complex baseband lowpass filter can be used as the band-limiting function and inserted into the basis function of the original model, which can be conducted by using linear convolution. The new band-limited model can therefore be written as,

$$\begin{aligned}\tilde{u}(n) = &\sum_{p=0}^{(P-1)/2}\sum_{i=0}^{M}\tilde{g}_{2p+1,1,BL}(i)\left[\sum_{k=0}^{K}|\tilde{x}(n-k)|^{2p}\tilde{x}(n-i-k)\tilde{w}(k)\right]\\ &+\sum_{p=1}^{(P-1)/2}\sum_{i=1}^{M}\tilde{g}_{2p+1,2,BL}(i)\left[\sum_{k=0}^{K}|\tilde{x}(n-k)|^{2(p-1)}\tilde{x}^2(n-k)\tilde{x}^*(n-i-k)\tilde{w}(k)\right]\\ &+\sum_{p=1}^{(P-1)/2}\sum_{i=1}^{M}\tilde{g}_{2p+1,3,BL}(i)\left[\sum_{k=0}^{K}|\tilde{x}(n-k)|^{2(p-1)}\tilde{x}(n-k)\,|\tilde{x}(n-i-k)|^2\,\tilde{w}(k)\right]\\ &+\sum_{p=1}^{(P-1)/2}\sum_{i=1}^{M}\tilde{g}_{2p+1,4,BL}(i)\left[\sum_{k=0}^{K}|\tilde{x}(n-k)|^{2(p-1)}\tilde{x}^*(n-k)\tilde{x}^2(n-i-k)\tilde{w}(k)\right]\end{aligned} \tag{22}$$

where $\tilde{w}(\cdot)$ is the baseband band-limiting function with length K, $\tilde{g}_{2p+1,j,BL}(\cdot)$ is the band-limited complex Volterra kernel of the system.

In matrix form, the new model can be represented as

$$\mathbf{U}_{N\times 1} = \mathbf{X}_{N\times L}\mathbf{C}_{L\times 1} \tag{23}$$

where N is the number of data samples and L is the number of coefficients. $\mathbf{C}$ is the coefficients matrix containing all coefficients,

$$\mathbf{C}_{L\times 1} = \left[\tilde{g}_{1,1,BL}(0) \quad \dots \quad \tilde{g}_{3,1,BL}(1) \quad \dots\right]^T, \tag{24}$$

and $\mathbf{U}$ is the output matrix generated from the predistorted input $\tilde{u}(n)$,

$$\mathbf{U}_{N\times 1} = \left[\tilde{u}(n) \quad \tilde{u}(n-1) \quad \dots \quad \tilde{u}(n-N+1)\right]^T. \tag{25}$$

$\mathbf{X}$ is the input matrix generated from the original input $\tilde{x}(n)$, containing all linear and nonlinear terms appearing in the input of the model represented by (22), which can be formed as

$$\mathbf{X}_{N\times L} = \begin{bmatrix} \sum_{k=0}^{K}\tilde{x}(n-k)\tilde{w}(k) & \dots & \sum_{k=0}^{K}|\tilde{x}(n-k)|^2\,\tilde{x}(n-1-k)\tilde{w}(k) & \dots \\ \sum_{k=0}^{K}\tilde{x}(n-1-k)\tilde{w}(k) & \dots & \sum_{k=0}^{K}|\tilde{x}(n-1-k)|^2\,\tilde{x}(n-2-k)\tilde{w}(k) & \dots \\ \vdots & \vdots & \vdots & \vdots \\ \sum_{k=0}^{K}\tilde{x}(n-N+1-k)\tilde{w}(k) & \dots & \sum_{k=0}^{K}|\tilde{x}(n-N+1-k)|^2\,\tilde{x}(n-N-k)\tilde{w}(k) & \dots \end{bmatrix} \tag{26}$$

As described in [21], a single function based DPD may not be sufficient to linearize some types of RF PAs, e.g., envelope tracking or multistage Doherty amplifiers. The vector decomposition technique [21] can then be used to form a decomposed piecewise Volterra model to characterize a wider range of nonlinear systems. In the band-limited case, this technique can also be directly applied.

B. Model Parameter Extraction

To extract the coefficients, the indirect learning [18][19] can be employed, where the feedback signal, i.e., the output of the PA, $\tilde{y}(n)$, is used as the input of the model, while the predistorted input signal, $\tilde{u}(n)$, is used as the expected output. By employing the standard least squares algorithm, the coefficients vector $\mathbf{C}$ can be estimated from,

$$\hat{\mathbf{C}}_{L\times 1} = [(\mathbf{Y}^H)_{L\times N}\mathbf{Y}_{N\times L}]^{-1}(\mathbf{Y}^H)_{L\times N}\mathbf{U}_{N\times 1} \tag{27}$$

where $\hat{\mathbf{C}}$ is the extracted coefficients with length L. $\mathbf{Y}$ is constructed from the PA output $\tilde{y}(n)$ in the same way of $\mathbf{X}$, and $\mathbf{U}$ is the expected inverse output matrix generated from the PA input (the output of the predistorter), $\tilde{u}(n)$. In the first iteration, $\tilde{u}(n)$ is equal to $\tilde{x}(n)$.

V. Experimental Results

In this section, the performance of band-limited Volterra DPD will be validated in several experimental tests. A high power LDMOS Doherty PA operated at 2.14 GHz was used. The test bench was set up as shown in Fig. 8. A baseband I/Q complex signal source is generated in MATLAB from PC and sent into the baseband board. The baseband signal is first converted into the analog domain, and then modulated and up-converted to the RF frequency. The signal then passes a driver and is finally fed into the main PA. In the feedback loop, the output of the PA is down-converted to baseband and captured back to the PC. The baseband I/Q data sampling rate is 184.32 MSPS and the system bandwidth is limited to 140 MHz. Due to hardware limitations, we could not arbitrarily change the analog filter bandwidth on the PA output or the sampling rate of data converters. To vary the system bandwidth, we processed the signal in the digital domain to emulate the bandwidth changes in the analog domain instead. For instance, in the 80 MHz case, we filtered the 140 MHz signal captured from the bench to 80 MHz in the digital domain before

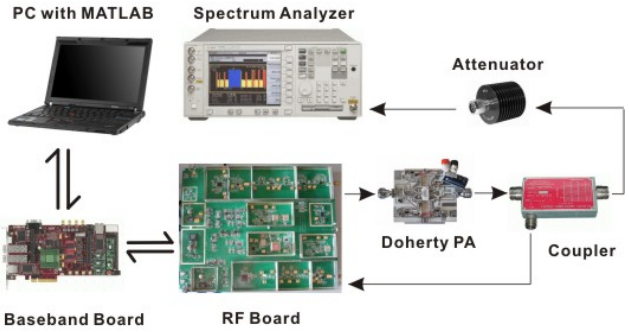

Fig. 8. Experimental test bench setup.

conducting the model extraction and digital predistortion. The performance should match that of the physical changes in a real system, although other factors may need to be considered, e.g., noise floor of the ADCs and filters. But for verifying the idea proposed in this paper, it does not make much difference.

A. Proposed Model vs. Conventional Model

In order to validate the linearization performance, we first compared the proposed DPD model with the conventional DPD model. The test was conducted in three scenarios: (i) the conventional model with a sufficient bandwidth; (ii) the conventional model with a limited bandwidth; (iii) the proposed model with a limited bandwidth. A 20 MHz 4-carrier WCDMA signal with PAPR (peak-to-average power ratio) of 6.5 dB was used to excite the PA with an average output power at 36 dBm. In the sufficient bandwidth scenario, the system bandwidth was set to 140 MHz, which was 7 times the input signal bandwidth. Therefore, almost all the distortions caused by the PA nonlinearities and memory effects were captured. In the band-limited scenarios, the system bandwidth was set to only 2 times the input bandwidth, i.e., 40 MHz. The DPD model employed was the decomposed piecewise 2nd-order DDR model discussed in section IV. The magnitude threshold was set as 0.5 for the normalized data, the corresponding nonlinearity order was selected as {7,7}, and the memory length was set to {3,3}. In theory, the band-limiting function in the proposed model should be an ideal rectangular filter, but in practice, it can be a normal FIR filter, and the order and the type of the filter can be chosen according to the real system performance requirement. In this test, an equiripple lowpass filter was chosen, and its bandwidth was set to 40 MHz. To eliminate the effects induced by the filter, we used a very high order filter with 266 coefficients in the initial test, but the order of the filter was reduced in the late test for other performance evaluations.

The test results are shown in Table I, and the frequency domain spectra are plotted in Fig. 9. We can see that the conventional model can achieve excellent performance when a sufficient linearization bandwidth is provided. 30 dB ACPR (adjacent channel power ratio) reduction can be obtained and NMSE (normalized mean square errors) is reduced from -21 dB to -46 dB. However, when the system bandwidth is reduced, the performance of the conventional model is dramatically deteriorated, 9 dB and 15 dB worse in ACPR with 5 and 10 MHz frequency offset, respectively, when the DPD bandwidth is reduced from 140 MHz to 40 MHz. However, if the proposed

TABLE I
PERFORMANCE FOR 20 MHZ 4-CARRIER WCDMA SIGNAL

	BW (MHz)	NMSE (dB)	ACPR (dBc) ±5 MHz	ACPR (dBc) ±10 MHz
Without DPD	140	-21.13	-29.72/-28.40	-32.05/-29.96
Conventional DPD	140	-46.34	-60.41/-61.51	-61.91/-62.82
	40	-38.15	-51.25/-52.27	-46.61/-47.04
Proposed DPD	40	-45.83	-61.20/-59.83	-60.44/-60.40

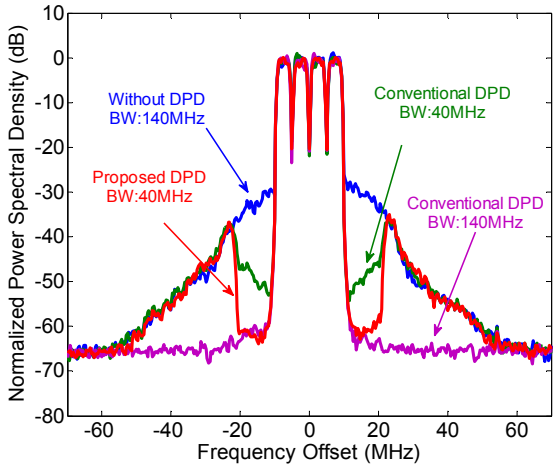

Fig. 9. Output spectra in comparison between the proposed model and the conventional model.

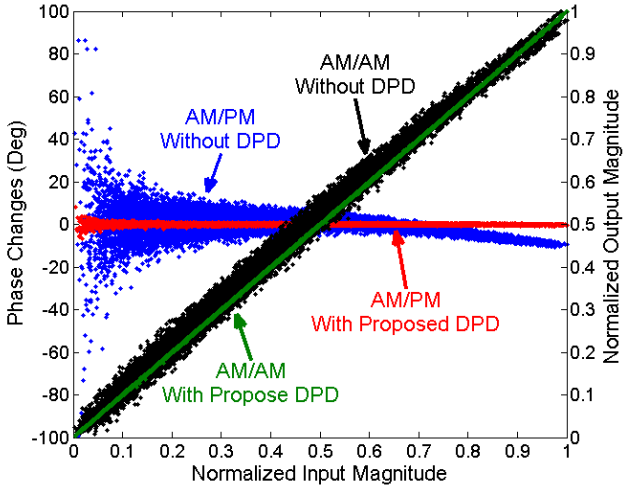

Fig. 10. AM/AM and AM/PM characteristics with/without proposed DPD for a 4-carrier 20 MHz WCDMA signal with 40 MHz linearization bandwidth.

DPD is employed, almost the same performance can be achieved as that of the conventional model within the selected linearization bandwidth. After filtering, the original signal can be restored. Fig. 10 shows the AM/AM and AM/PM characteristics before and after the proposed DPD, where we can see that the distortion caused by the PA nonlinearities and memory effects can be effectively removed.

B. Performance with Various Linearization Bandwidths

In Section V.A, we compared the performance produced by the proposed model with that by the conventional model within

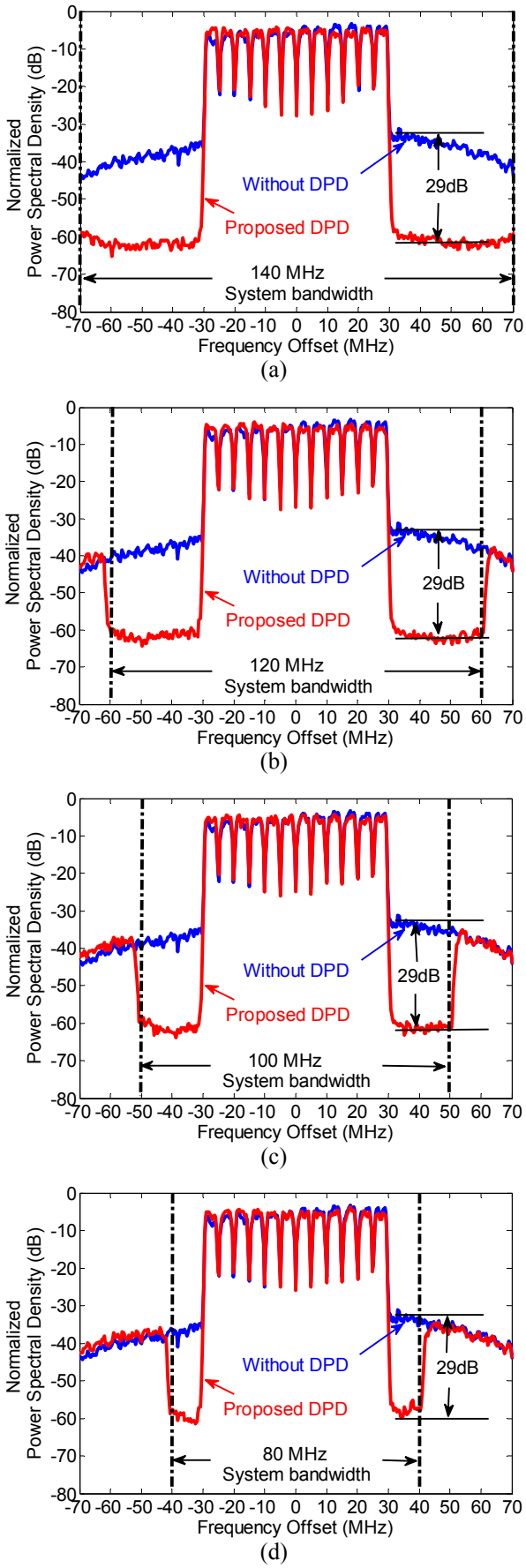

Fig. 11. Output spectra under different linearization bandwidths: (a) 140 MHz, (b) 120 MHz, (c) 100 MHz, and (d) 80 MHz.

a fixed bandwidth. In this section, we verify how the system bandwidth changes affect the linearization performance. In this test, a 60 MHz 12-carrier UMTS signal with PAPR of 6.5 dB was used to excite the PA and again with an average output power at 36 dBm. The same model was used as that in Section A, except the memory length was set to {5,5}. The system bandwidth was varied from 140 MHz to 80 MHz. The bandwidth of the band-limiting function was set to the correspondent system bandwidth, and the order of the filter was reduced to 82.

The spectra of the PA output with and without DPD are plotted in Fig. 11, where we can see that the linearization performance is kept almost the same, with 29 dB improvement in ACPR, within the selected bandwidth from 140 MHz to 80 MHz. It can be further verified by calculating the NMSE and ACPR values under the different system bandwidths. As presented in Fig. 12, both NMSE and ACPR values only fluctuated within a very small range. This test result confirms that the system bandwidth changes do not affect the linearization performance as long as the DPD model bandwidth matches the system under modeling, which also verifies the conclusion made in the Section III.B.

C. Performance with Various Signal Configurations

In this section, we employ the proposed DPD model to linearize a system excited with further wider band signals and with different signal configurations, e.g., 100 MHz signals in three scenarios: (i) 5-carrier LTE-Advanced signal with contiguous configuration and with PAPR of 7.8 dB; (ii) 3-carrier LTE-Advanced signal with non-contiguous configuration and with PAPR of 7.7 dB; (iii) LTE-Advanced + UMTS mixed-mode signal with PAPR of 9.2 dB.

The configurations for the DPD model were the same as that in Section V.B, except that the bandwidth is fixed at 140 MHz. Fig. 13 shows the frequency domain spectra in three scenarios and the NMSE and ACPR values are listed in Table II. From these results we can see that the conventional model did not perform well, while the proposed model could consistently achieve excellent performance. From the spectra, we can clearly see that not only the out-of-band distortion was reduced but also the in-band distortion was cleaned up. It again verifies the conclusion made earlier. To the authors' knowledge, this is the first high performance linearization result for 100 MHz signals published to date.

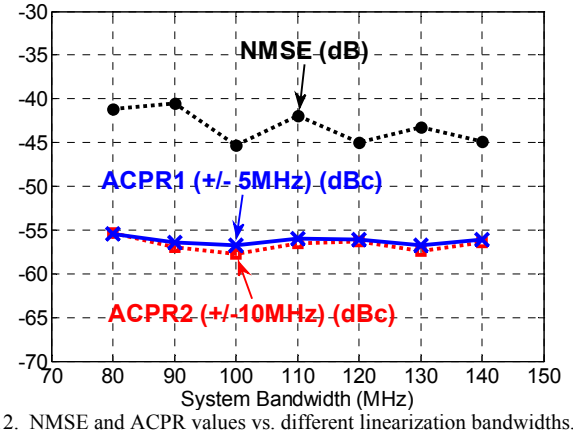

Fig. 12. NMSE and ACPR values vs. different linearization bandwidths.

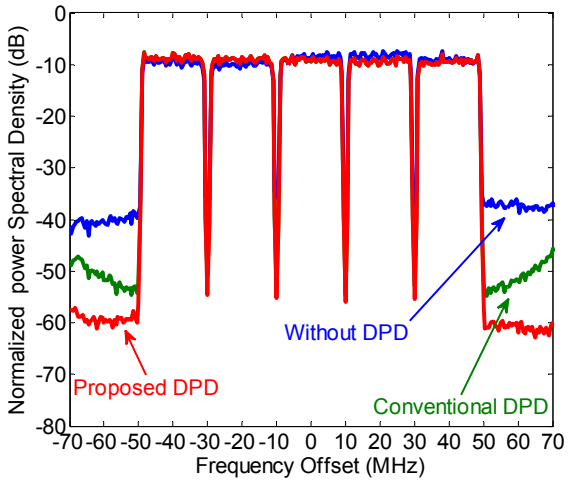

(a)

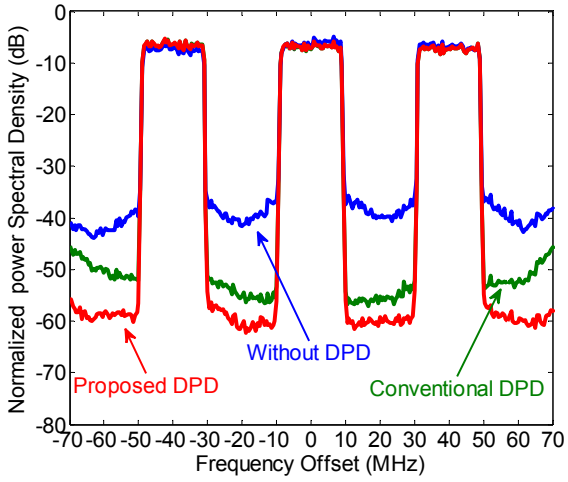

(b)

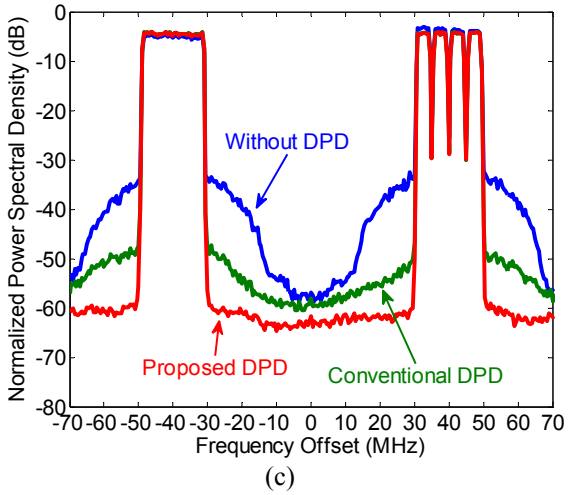

(c)

Fig. 13. Output spectra under different scenarios: (a) scenario 1, (b) scenario 2, and (c) scenario 3.

TABLE II
PERFORMANCE FOR 100 MHZ SIGNALS

	NMSE (dB)	ACPR (dBc) (±20 MHz)
Scenario 1		
Without DPD	-17.35	-30.69/-27.82
Conventional DPD	-33.48	-42.80/-43.27
Proposed DPD	-41.66	-51.02/-52.22
Scenario 2		
Without DPD	-18.84	-35.31/-33.22
Conventional DPD	-35.51	-42.74/-44.07
Proposed DPD	-41.94	-52.57/-53.44
Scenario 3		
Without DPD	-17.21	-34.61/-33.08
Conventional DPD	-36.88	-46.23/-47.67
Proposed DPD	-43.53	-56.14/-57.04

VI. CONCLUSION

In this paper, a novel band-limited Volterra series-based behavioral model and its related DPD system have been presented. Theoretical analysis and experimental results showed that this new band-limited modeling technique not only significantly improves the model accuracy but more importantly, it eliminates the system bandwidth constraints of the conventional DPD techniques. It provides an extra freedom for DPD designers to arbitrarily choose the bandwidth to be linearized in the PA output according to the system requirement without sacrificing performance, which makes the system design much more flexible and practical. Furthermore, this modeling technique is very general. It is not limited to the Volterra series-based models that we presented in this paper, but it also can be applied to other linear-in-parameters models. In future ultra wideband systems, this new technique can significantly improve system performance and reduce DPD implementation cost. We expect that this technique will make significant impact in the digital predistortion field.

REFERENCES

[1] T. Ali-Yahiya, *Understanding LTE and its Performance*, Springer, New York, 2011.

[2] P. B. Kennington, *High Linearity RF Amplifier Design*, Norwood, MA: Artech House, 2000.

[3] F. Luo, *Digital Front-End in Wireless Communications and Broadcasting*, Cambridge University Press, Cambridge, UK, 2011.

[4] F. M. Ghannouchi, and O. Hammi, "Behavioral modeling and predistortion," *IEEE Microwave Mag.,* vol. 10, no. 7, pp. 52-64, Dec. 2009.

[5] J. Kim, and K. Konstantinou, "Digital predistortion of wideband signals based on power amplifier model with memory," *Electron. Lett.*, vol. 37, no. 23, pp. 1417–1418, Nov. 2001.

[6] D. R. Morgan, Z. Ma, J. Kim, M. G. Zierdt, and J. Pastalan, "A generalized memory polynomial model for digital predistortion of RF power amplifiers," *IEEE Trans. Signal Process.*, vol. 54, no. 10, pp. 3852–3860, Oct. 2006.

[7] A. Zhu, J. C. Pedro, and T. J. Brazil, "Dynamic deviation reduction based Volterra behavioral modeling of RF power amplifiers," *IEEE Trans. Microw Theory Tech.*, vol. 54, no. 12, pp. 4323–4332, Dec. 2006.

[8] A. Zhu, P. J. Draxler, J. J. Yan, T. J. Brazil, D. F. Kinball, and P. M. Asbeck, "Open-loop digital predistorter for RF power amplifiers using

dynamic deviation reduction-based Volterra series," *IEEE Trans. Microw. Theory Tech*, vol. 56, no. 7, pp. 1524–1534, Jul. 2008.

[9] S. Hong, Y. Y. Woo, J. Kim, J. Cha, I. Kim, J. Moon, J. Yi, and B. Kim, "Weighted polynomial digital predistortion for low memory effect Doherty power amplifier," *IEEE Trans. Microw. Theory Tech*., vol. 55, no. 5, pp. 925–931, May 2007.

[10] T. Liu, S. Boumaiza, and F. M. Ghannouchi, "Augmented Hammerstein predistorter for linearization of broadband wireless transmitters," *IEEE Trans. Microw. Theory Tech*., vol. 54, no. 4, pp. 1340–1349, Jun.2006.

[11] J. Kim, Y. Y. Woo, J. Moon, and B. Kim, "A new wideband adaptive digital predistortion technique employing feedback linearization," *IEEE Trans. Microw. Theory Tech*, vol. 56, no. 2, pp. 385-392, Feb. 2008.

[12] N. Safari, T. Røste, P. Fedorenko, and J. S. Kenny, "An approximation of Volterra series using delay envelopes, applied to digital predistortion of RF power amplifiers with memory effects," *IEEE Microw. Wireless Compon. Lett*., vol. 18, no. 2, pp. 115–117, Feb. 2008.

[13] O. Hammi, S. Carichner, B. Vassilakis, and F. M. Ghannouchi, "Synergetic crest factor reduction and baseband digital predistortion for adaptive 3G Doherty power amplifier linearizer Design," *IEEE Trans. Microw. Theory Tech*, vol. 56, no. 11, pp. 2602-2608, Nov. 2008.

[14] S. A. Bassam, W. Chen, M. Helaoui, F. M. Ghannouchi, Z. Feng, "Linearization of concurrent dual-band power amplifier based on 2D-DPD technique," *IEEE Microw. Wireless Compon. Lett.*, vol. 21, no. 12, pp. 685-687, Dec. 2011.

[15] H. Cao, H. M. Nemati, A. S. Tehrani, T. Eriksson, and C. Fager, "Digital predistortion for high efficiency power amplifier architectures using a dual-input modeling approach," *IEEE Trans. Microw. Theory Tech.*, vol. 60, no. 2, pp. 361-369, Feb. 2012.

[16] C. Yu, L. Guan, and A. Zhu, "Band-limited Volterra series-based behavioral modeling of RF power amplifiers," in *IEEE MTT-S Int. Microw. Symp. Dig.*, Montreal, Canada, Jun. 2012.

[17] M. Schetzen, *The Volterra and Wiener Theories of Nonlinear Systems*, reprint ed. Melbourne, FL: Krieger, 1989.

[18] C. Eun and E. J. Powers, "A new Volterra predistorter based on the indirect learning architecture," *IEEE Trans. Signal Process.*, vol. 45, no. 1, pp. 223–227, Jan. 1997.

[19] L. Ding, G. T. Zhou, D. R. Morgan, Z. Ma, J. S. Kenney, J. Kim, and C. R. Giardina, "A robust digital baseband predistorter constructed using memory polynomials," *IEEE Trans. Commun*., vol. 52, no. 1, pp. 159 – 165, Jan. 2004.

[20] L. Guan, and A. Zhu, "Simplified dynamic deviation reduction-based volterra model for Doherty power amplifiers," presented at *the IEEE Int. Integr. Nonlinear Microw. Millimeter-Wave Circuits Workshop*, Vienna, Austria, Apr. 2011.

[21] A. Zhu , P. J. Draxler , H. Chin , T. J. Brazil , D. F. Kimball, and P. M. Asbeck, "Digital predistortion for envelope-tracking power amplifiers using decomposed piecewise Volterra series", *IEEE Trans. Microw. Theory Tech.*, vol. 56, no. 10, pp. 2237-2247 , Oct. 2008.

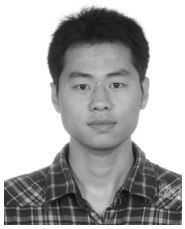

Chao Yu (S'09) received the B.E. and M.E. degree from School of Information Science and Engineering, Southeast University, Nanjing, China, in 2007 and 2010, respectively. He is currently working toward the Ph.D. degree at University College Dublin, Dublin, Ireland.

His research interests include antenna design, behavioral modeling and digital predistortion for RF power amplifiers.

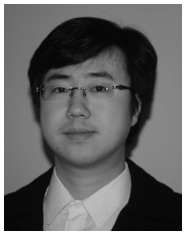

Lei Guan (S'09) received the B.E. degree and the M.E. degree, both in Electronic Engineering from Harbin Institute of Technology (HIT), Harbin, China in 2006 and 2008, respectively. He was awarded the Ph.D. degree in Electronic Engineering in 2012 by University College Dublin (UCD), Dublin, Ireland. He is currently working as a Senior Research Engineer with School of Electrical, Electronic and Communications Engineering at UCD, Ireland.

His research interests include linearization and system-level modeling of RF/Microwave power amplifiers with emphasis on digital predistortion (DPD) based PA linearization and its FPGA hardware implementation. He also has interests in nonlinear system identification algorithms, digital signal processing (DSP), wireless communication system design and FPGA-based parallel computing.

Erni Zhu, photograph and biography are not available at time of publication.

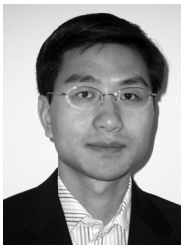

Anding Zhu (S'00-M'04) received the B.E. degree in telecommunication engineering from NorthChina ElectricPower University, Baoding, China, in 1997, and the M.E. degree in computer applications from Beijing University of Posts and Telecommunications, Beijing, China, in 2000, and the Ph.D. degree in electronic engineering from University College Dublin (UCD), Dublin, Ireland, in 2004.

He is currently a Lecturer with the School of Electrical, Electronic and Communications Engineering, UCD. His research interests include high-frequency nonlinear system modeling and device characterization techniques with a particular emphasis on Volterra-series-based behavioral modeling and linearization for RF PAs. He is also interested in wireless and RF system design, digital signal processing and nonlinear system identification algorithms.